Electronic Supplementary Information

Photo-induced magnetic bistability in a controlled assembly of anisotropic coordination nanoparticles

Florence Volatron, Daniela Heurtaux, Laure Catala*, Corine Mathonière*, Alexandre Gloter, Odile Stéphan, Diego Repetto, Miguel Clemente-León*, Eugenio Coronado and Talal Mallah

-Structure of the coordination network $Cs^I{}_2Cu^{II}{}_7[Mo^{IV}(CN)_8]_4$, simulated from CIF file of reference 2

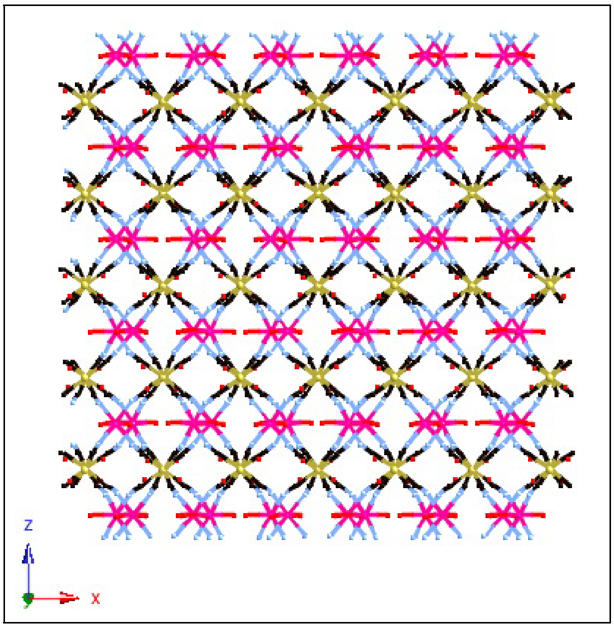

Mo in yellow Cu in pink, C in black, N in blue, O in red. Cs are omitted for the sake of clarity. For a detailed description of the structure see reference 2.

-Elemental analysis

compound	%	C	H	N	Cu	Mo	Cs
CsCuMo_DODA	**Exp.**	58,09	9,26	10,44	5 ,8	7,77	3,6
	Calc.[1]	58,08	9,32	10,78	6,11	7,91	3,65
CsMoCu_PVP	**Exp.**	56,38	7,88	11,59	0,95	0,93	1,12
	Calc.[2]	56,90	7,96	11,95	0,96	0,91	1,15

[1] **calculated for a composition of** $Cs_{0.5}Cu_{1.75}[Mo(CN)_8]_{1.5}[C_{38}H_{80}N]_2{\cdot}4.7H_2O$
[2] **calculated for a composition of** $Cs_1Cu_{1.75}[Mo(CN)_8]_{1.1}[C_6H_9NO]_{90}{\cdot}55.8H_2O$

In both cases the compostion of the inorganic core of the particles remains the same
The difference in Cs content between the two samples comes from the fact that in the PVP sample, the negatively charged particles have Cs^+ counter-cations, that are added to the Cs^+

cations inserted in the network. In the case of the **CsCuMo_DODA** sample DODA$^+$ cations replace the Cs$^+$ cations at the periphery of the particles. The difference in Mo(CN)8]$^{4-}$ comes from the fact that an amount of free DODA with diamagnetic [Mo(CN)8]$^{4-}$ coprecipitates with the particles, that cannot be washed off with any solvent.
Both analyses are helpful to determine (by comparison) the exact composition of the inorganic core.

-Preparation of the LB film (reproduced 3 times)

DODA dissolved in $CHCl_3$ was used as spreading solution. An appropriate amount of this solution was carefully spread onto the aqueous subphase of the nanoparticles prepared by diluting the original solution of the nanoparticles to a $3.7.10^{-5}$ M concentration of precursors, and the spreading solvent was allowed to evaporate for 10 minutes prior to compression. The monolayer was compressed up to a surface pressure of 30 mN/m for transfer. Multilayer LB films were assembled to the substrates by the vertical lifting method, i.e., immersion and withdrawal of the substrate through the interface covered with the film. The modified slide after emersion was dried with air previously to the next immersion, otherwise the transfer ratio decreased in the successive dipping cycles. The dipping speed of the substrates was 1 cm/min. ZnSe substrates were used for IR spectroscopy, hydrophilic glass substrates for AFM and mylar substrates for magnetic measurements. A KSV3000 trough was used to prepare the LB films. Millipore water with a resistivity higher than 18 MΩ cm was used in all the experiments.

Irradiation experiments:

Photomagnetic experiments were carried out with a Quantum Design MPMS-5S magnetometer working in the dc mode. The measurements were performed in the 2-300K range with magnetic field of 100 G and 5000 G, and at 2 K and 5 K up to 5 Teslas for magnetizations. The photomagnetic experiments were performed with a Ar^+-Kr^+ laser coupled through an optical fiber directed into the squid cavity for CsMoCu_PVP and the LB films, and with a 405 nm LED for CsMoCu_DODA. The output of the fiber is situated to a distance of 4 cm. Coated nanoparticles were laid down on the sample holder. The diamagnetic contribution and the weight were estimated by comparing the magnetization vs. magnetic field at 5K and χT curves measured in the 2-300K before irradiation with those recorded for the sample in a routine experiment (6,50 mg of sample loaded into a polymer bag). The irradiations experiments are conducted in the same manner for the DODA and PVP samples. The sequence measurements are the following : (a) in the dark : M=f(H) at 2 and 5 K, χ=f(T) at 100 Oe in the 2-100 K range and at 5000 Oe in the 2-300 K followed by M=f(H) at 2 and 5 K,, (b) irradiation at 480 nm for all samples except the CsMoCU_DODA sample that was studied at 405 nm , 10 K under 5000 Oe, (c) in the dark : M=f(H) at 2 and 5 K, M=f(T) under 100 Oe from 2 to 50 K, at 50 K, then anneal field to 0 Oe and go back to 5K, and measure again from 5 K to 50 K under 100 Oe (ZFC). For the LB film, the characterization is performed only during and after irradiation (as steps (b) and (c) described above).

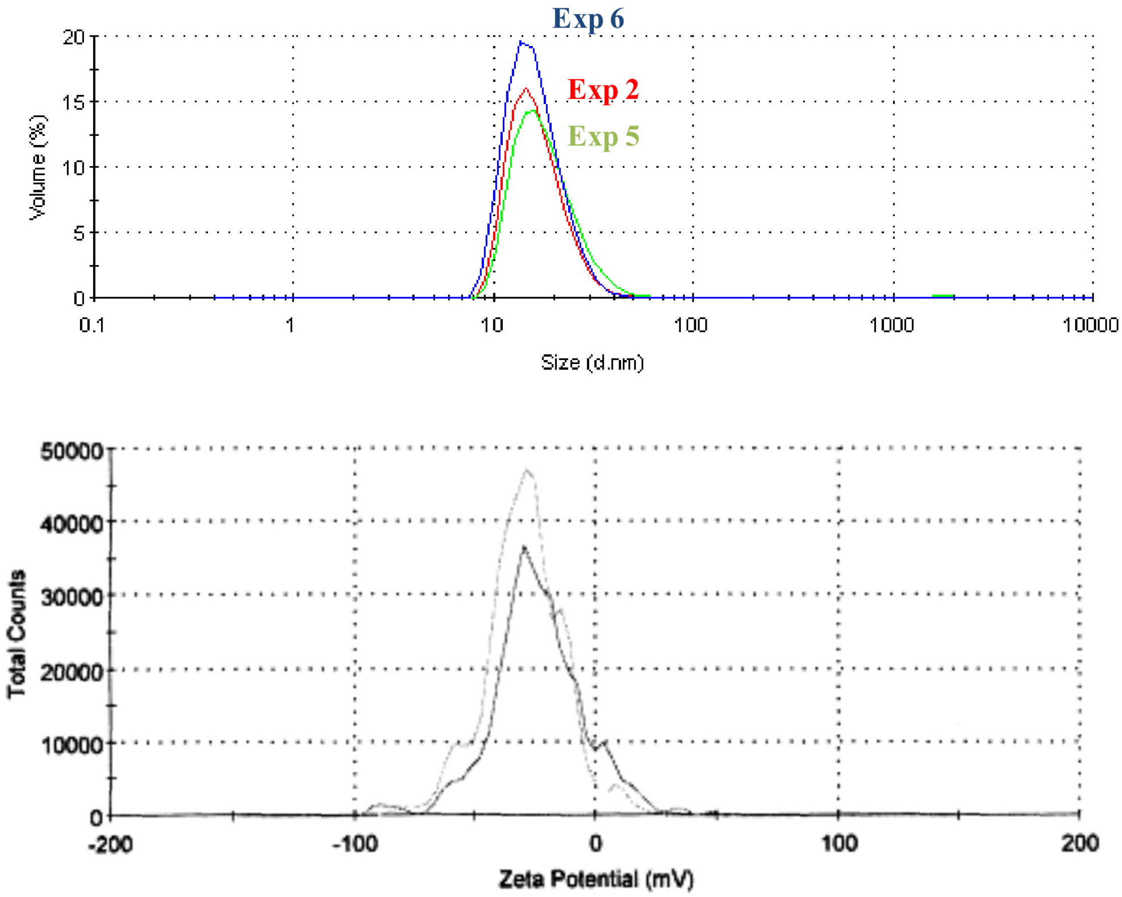

Fig. S1. Dynamic Light Scattering (top) obtained on three experiments with variable volumes exp 6 (V=300 mL), exp. 2 (V=50 mL) et exp. 5 (V=15 mL) and zeta potential measurements (bottom)

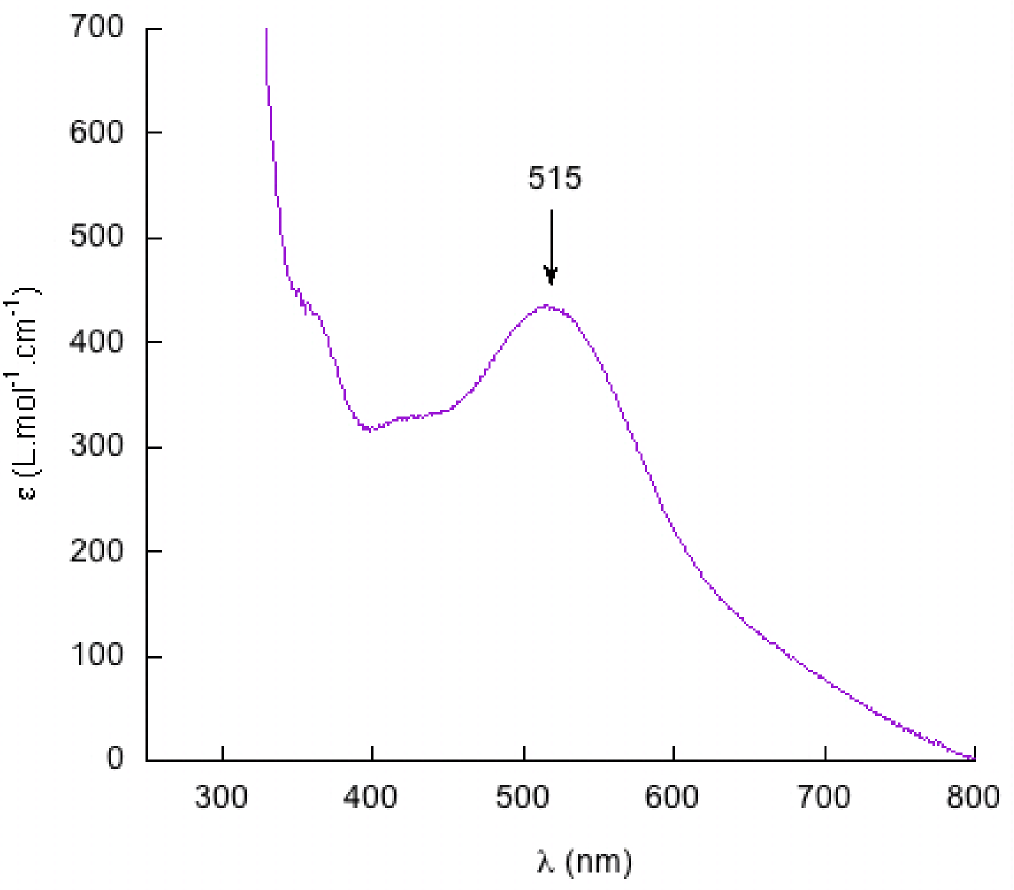

Fig. S2. UV-visible spectrum of the as-prepared water solution of nanoparticles.

The value of the absorption coefficient is ε= 435 L.mol^{-1}.cm^{-1} per $[Cs_{0.5}Cu^{II}_{1.75}[Mo^{IV}(CN)_8]_{1.1}]^{0.4-}$ formula unit , corresponding to the composition of the inorganic core. The concentration in $Cs_{0.5}Cu^{II}_{1.75}$ $[Mo^{IV}(CN)_8]_{1.1}]^{0.4-}$ entities is 5.7.10^{-4}M.

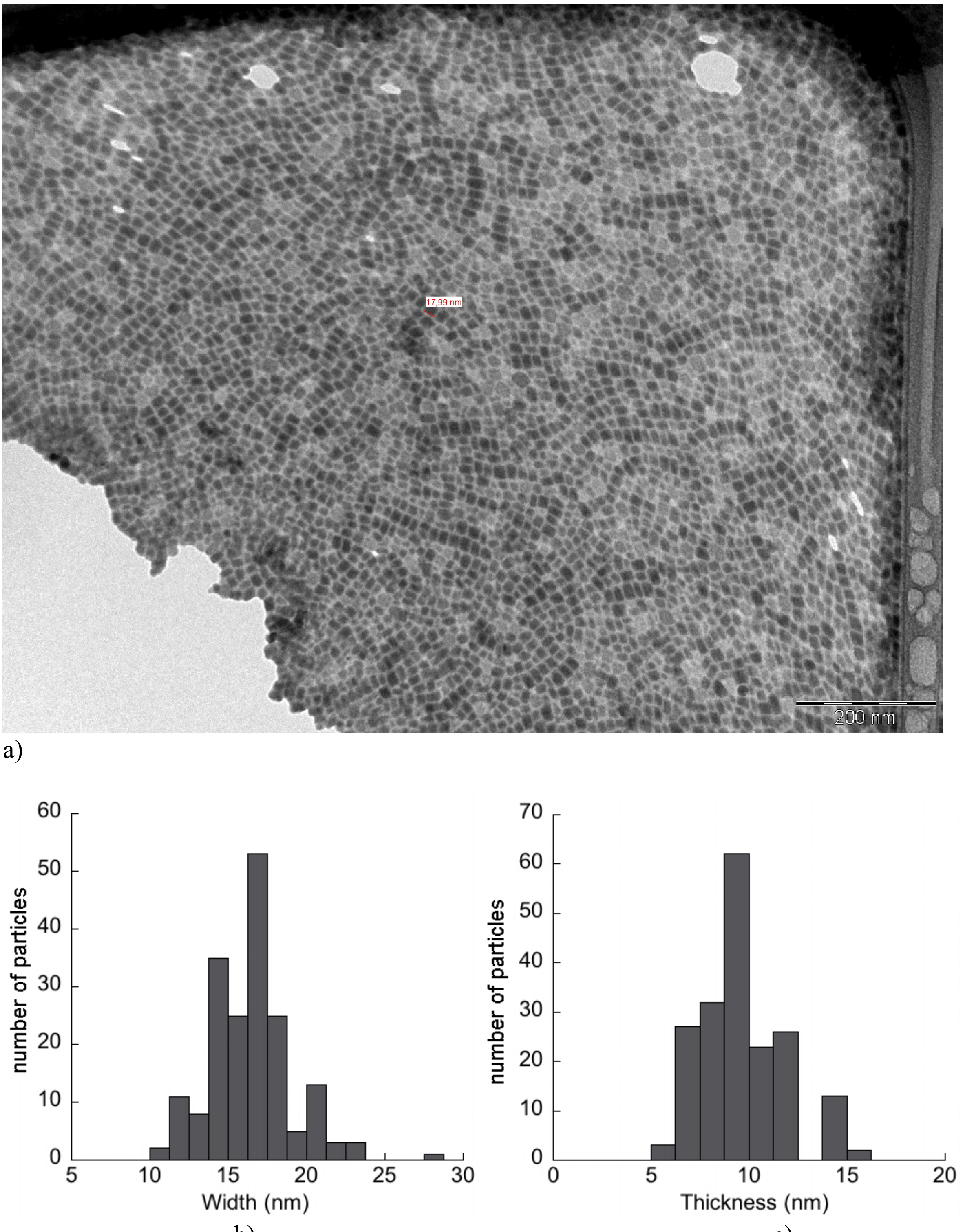

a)

b)

c)

Fig. S3. a) TEM image of the CSMoCu_DODA sample showing the stacking of most of the nanoparticles with their larger face perpendicular to the grid. b) Size distribution of the larger facets c) Size distribution of the thickness of the platelets.

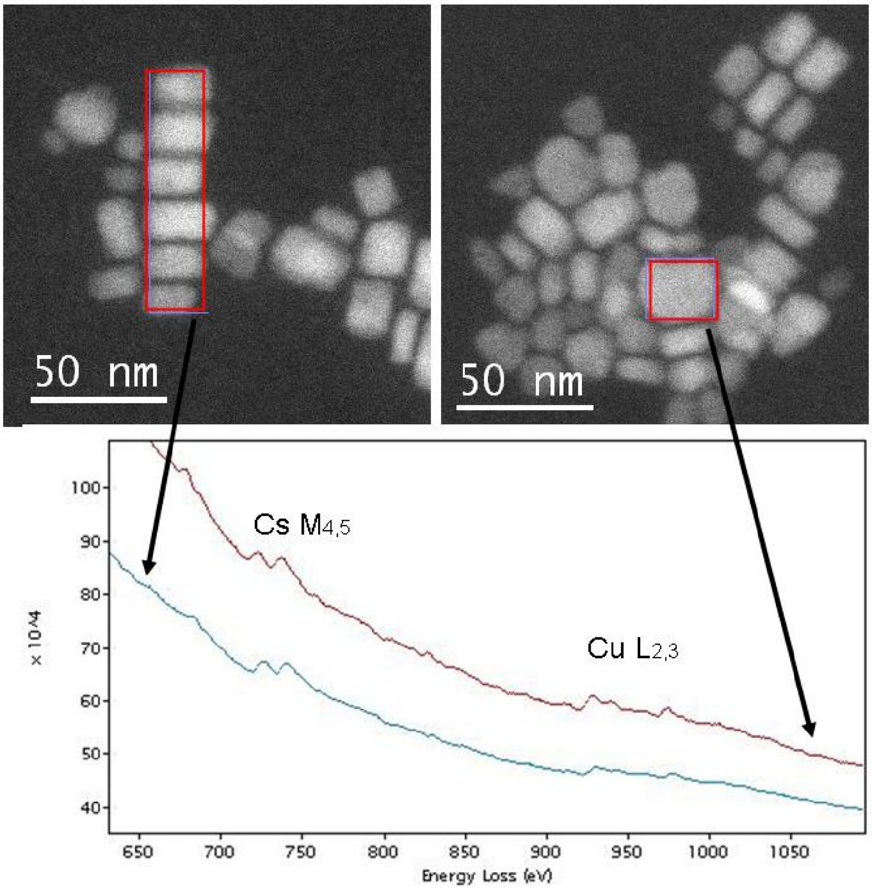

Fig. S4. EELS spectrum obtained on a column of particles stacked on their slice (left) and on a particle appearing as hexagon-like (right)

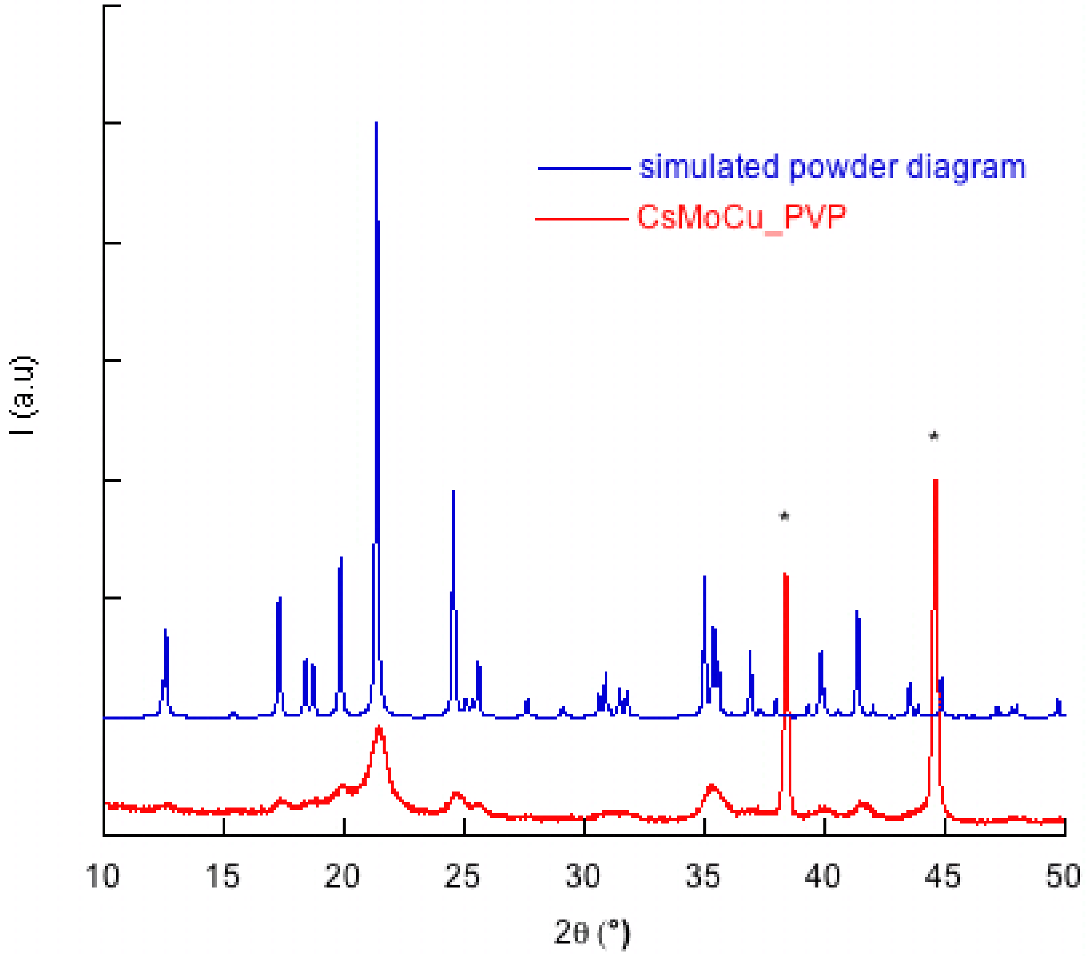

Fig. S5. X-Ray powder Diffraction diagram of the CsMoCu_DODA sample (top) and bulk (below, simulated with Powdercell software from structure of reference 2). The diffraction peaks are broadened due to the nanosized crystalline domains, leading to an overlapping of the diffraction peaks that precludes any size determination. The marked peaks (*) are due to the aluminium plate.

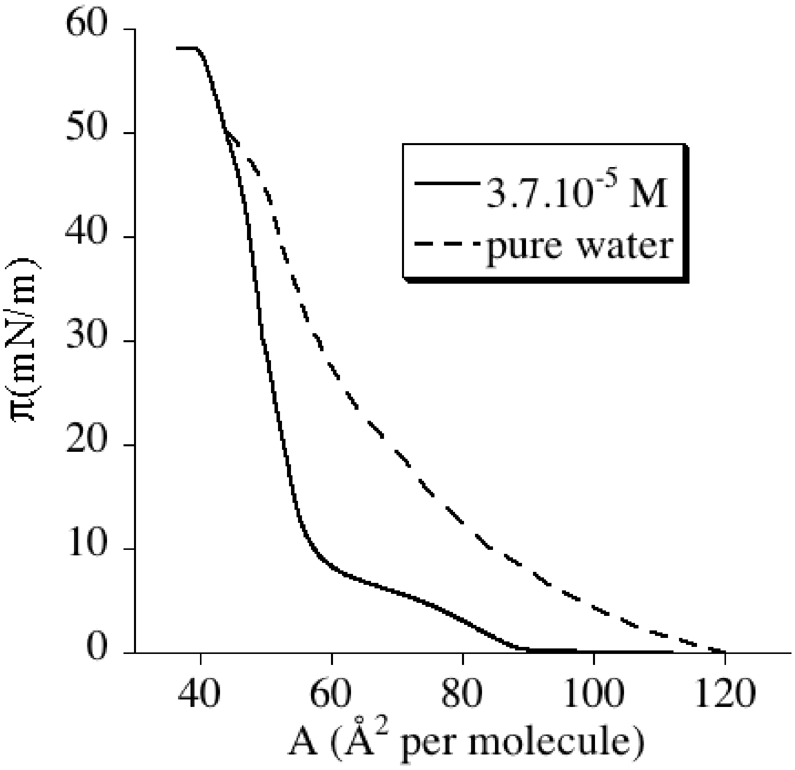

Fig. S6. Compression isotherm of DODA monolayer on a pure water (dotted line) subphase and a 3.7.10^{-5} M subphase (continuous line) of the nanoparticles.

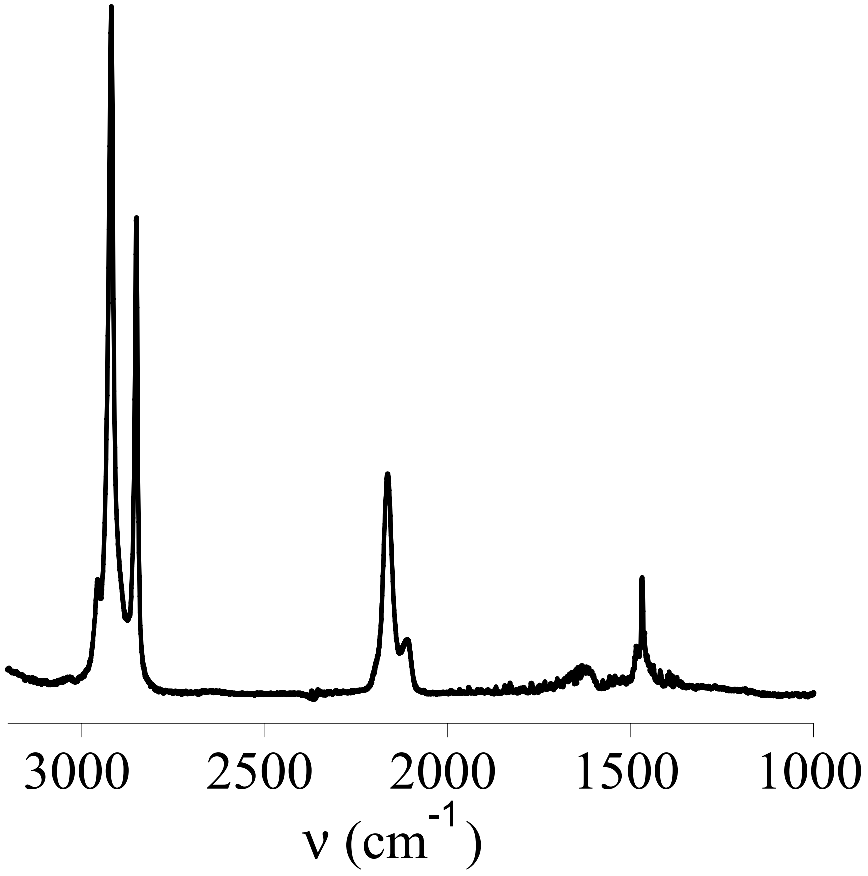

Fig. S7. IR spectrum of a LB Film of CsMoCu nanoparticles with 30 monolayers deposited on a ZnSe substrate.

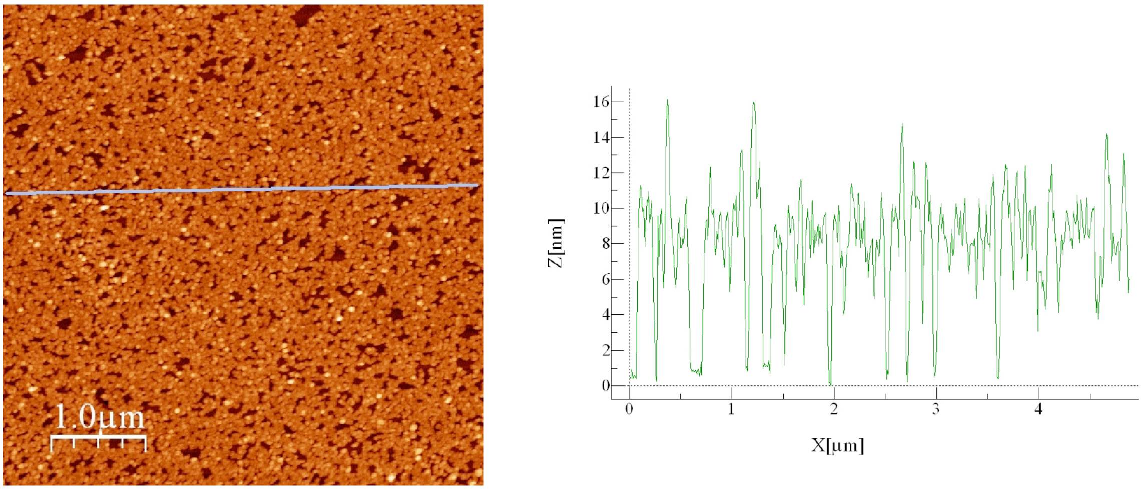

dense region

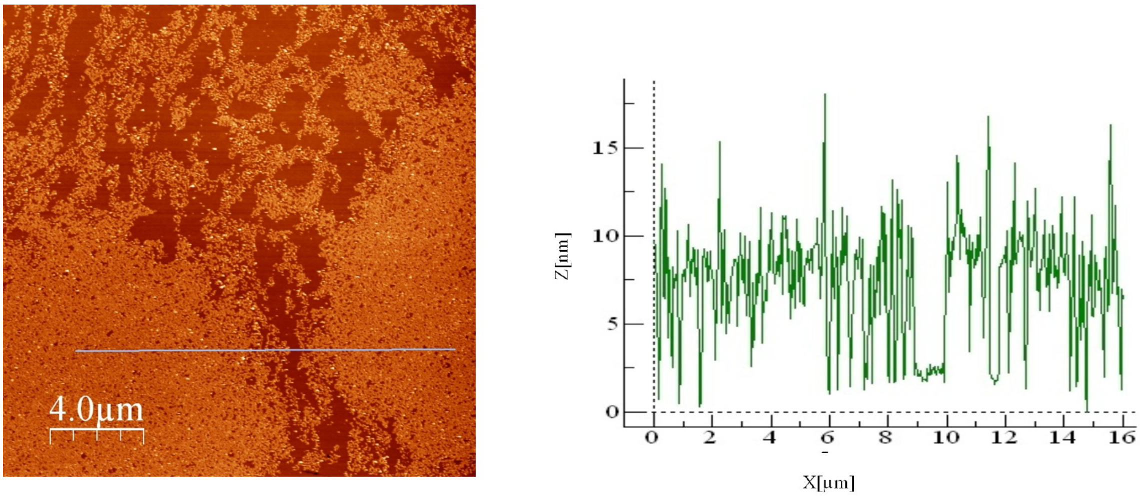

Larger scale

Fig. S8. Top) AFM profile obtained on the dense region on a micrometric scale on a LB film with one monolayer of the CSMoCu nanoparticles deposited on a glass substrate. Bottom) AFM profile obtained on a very large scale of the same LB film.

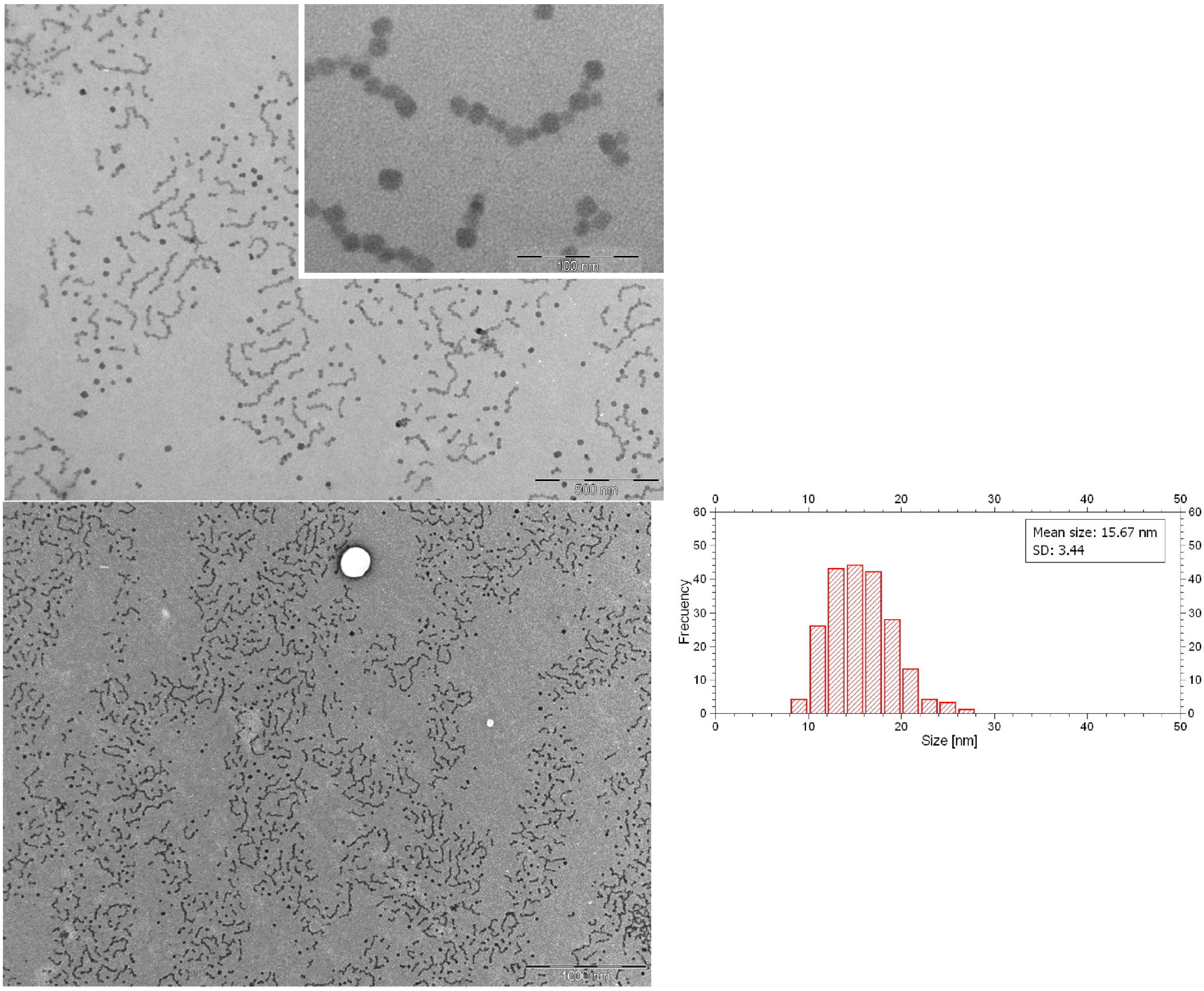

Fig. S9. Top) TEM image of a LB film with one monolayer deposited on a grid. Inset : zoom on some nanoparticles. Bottom) Large scale TEM image (scale=1 micron) of one layer of CsMoCu nanoparticles deposited on a grid and size distribution.

AFM measurements of LB films of 5 and 9 monolayers (ML) deposited on a glass substrate were also carried out in order to study how the morphology evolves in multilayer films. The total height of a pile formed by 5 nanoplatelets should be at least of 50 nm. By surface profiles it can be seen that for both 5 and 9 ML films the difference between the highest and the lowest point of the film is within 20 nm for most of the film. This means that the naked substrate is fully covered and just the two upmost monolayers are visible or, in other words, not complete. Moreover, since the difference between these two layers is mainly of 10 nm, the results show that the nanoplatelets maintain the preferential orientation, i.e. with the larger face parallel to the substrate, also in multilayers films.

The not perfect layer-by-layer growth can be basically attributed to the uncompleted coverage for each monolayer, already observed in the LB film with just one monolayer.

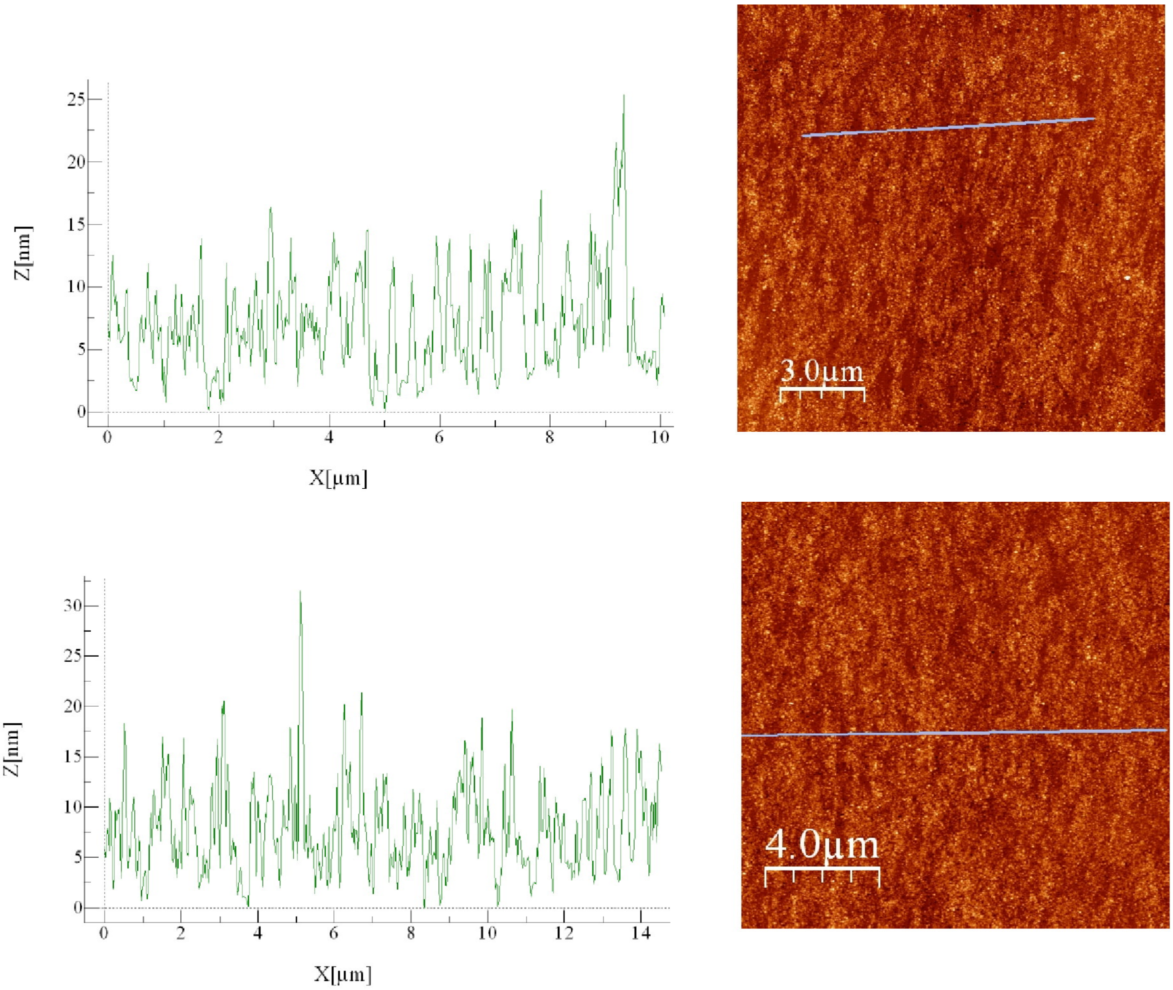

Fig. S10. AFM profile obtained on a micrometric scale on LB films with 5 and 9 monolayers of the CSMoCu nanoparticles deposited on a glass substrate.

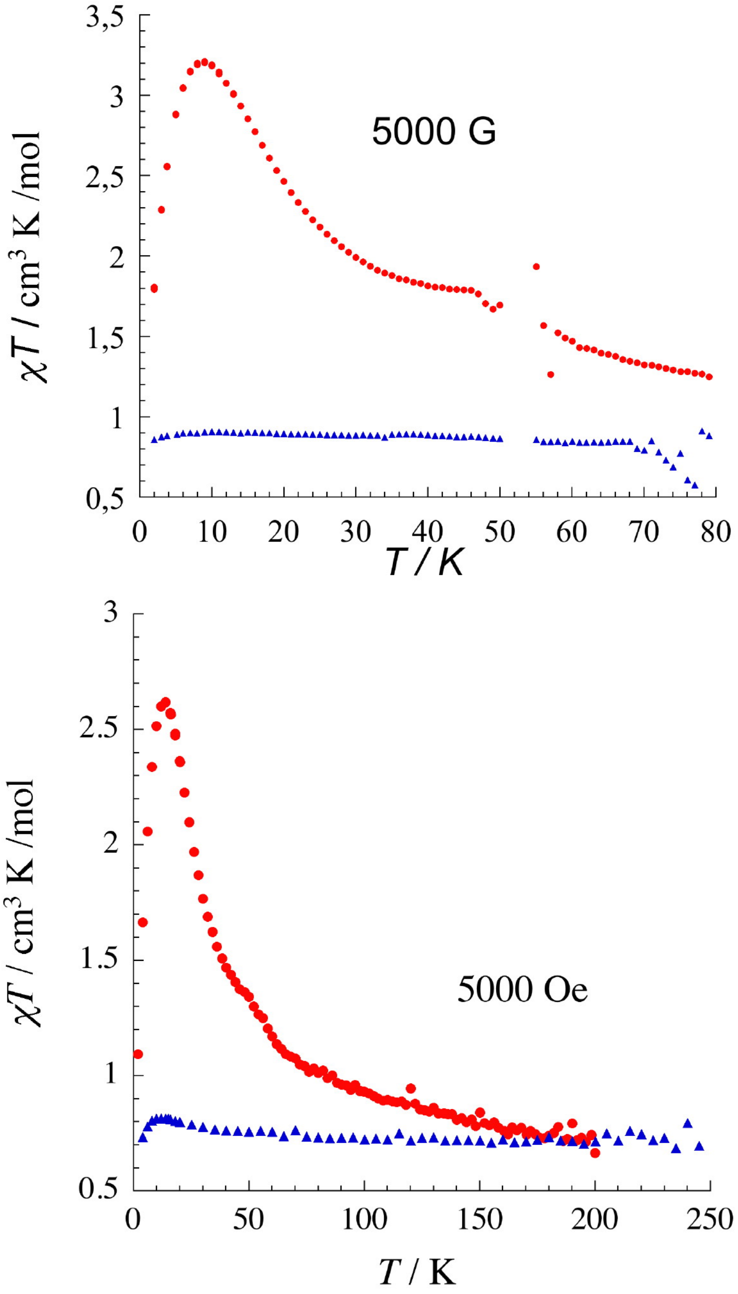

Fig. S11. χT = f(T) plot before (blue triangles) and after (red circles) irradiation for the CsMoCu_DODA sample (top)) and the CsMoCu_PVP sample (bottom)

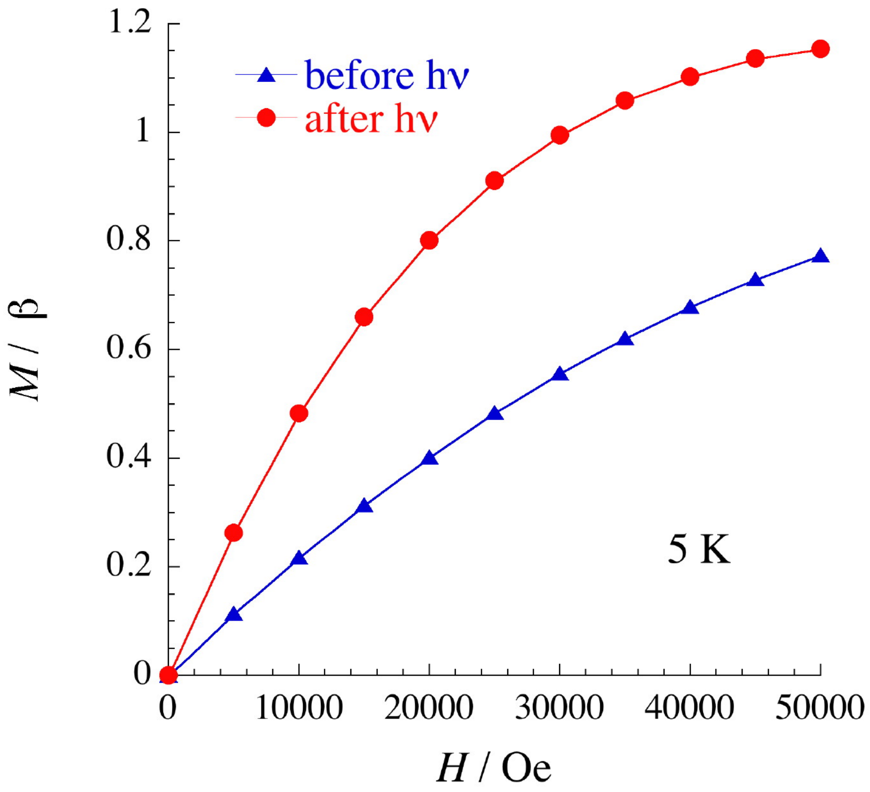

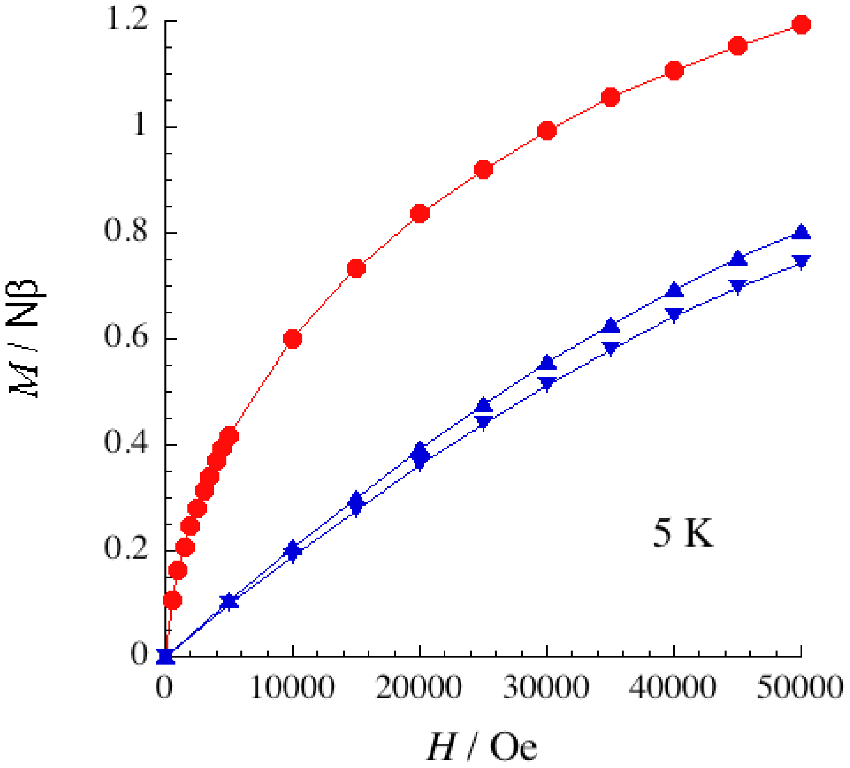

Fig. S12. M=f(H) plot measured at 5 K before (blue triangles) and after (red circles) irradiation for the CsMoCu_DODA sample (top) and the CsMoCu_PVP sample (bottom)

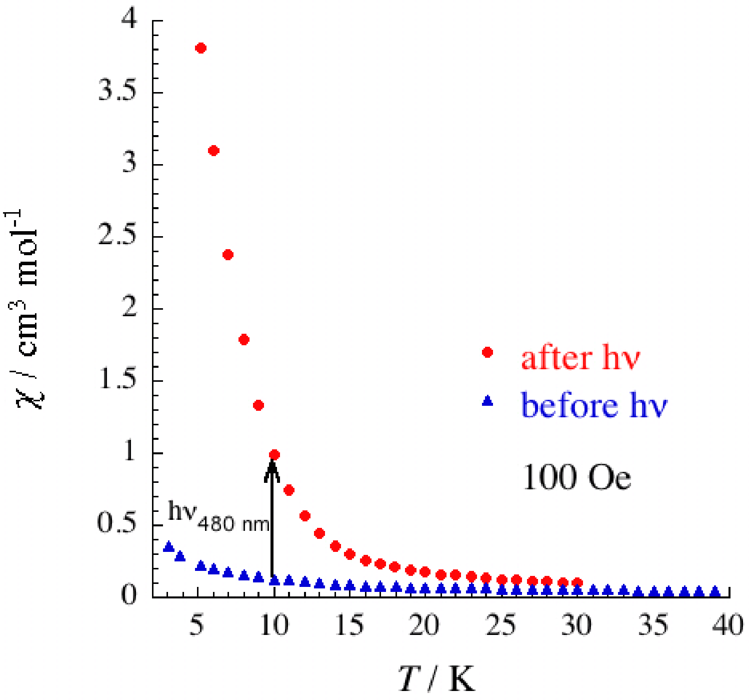

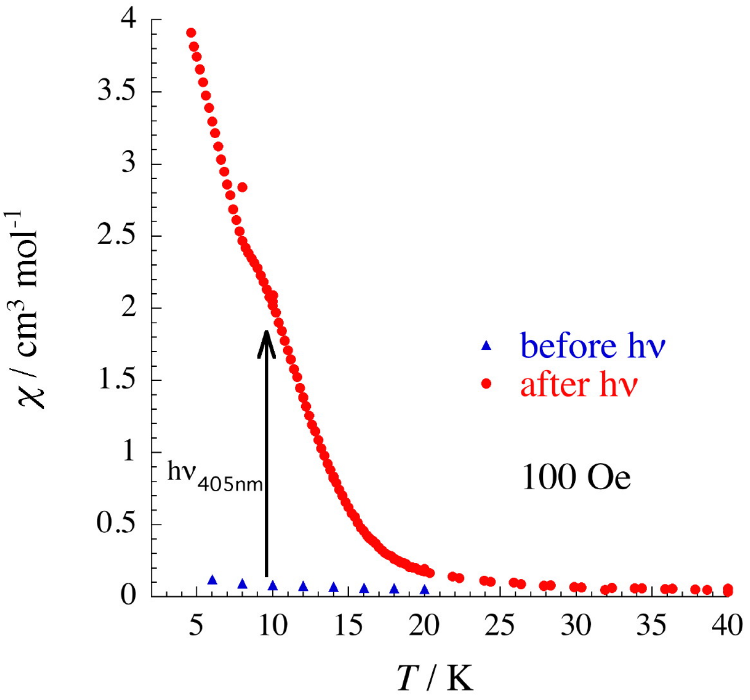

Fig. S13. Field-Cooled Magnetisations before (blue triangles) and after (red circles) irradiation for the CsMoCu_PVP sample (top)) and the CsMoCu_DODA sample (bottom) irradiated respectively at 480 and 405 nm.

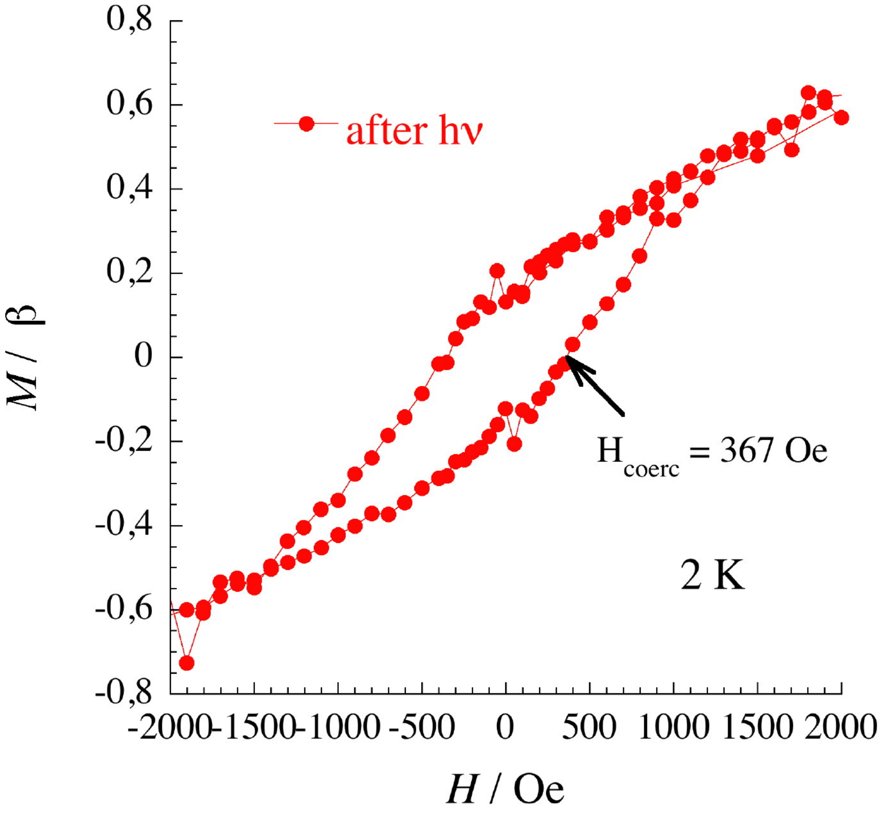

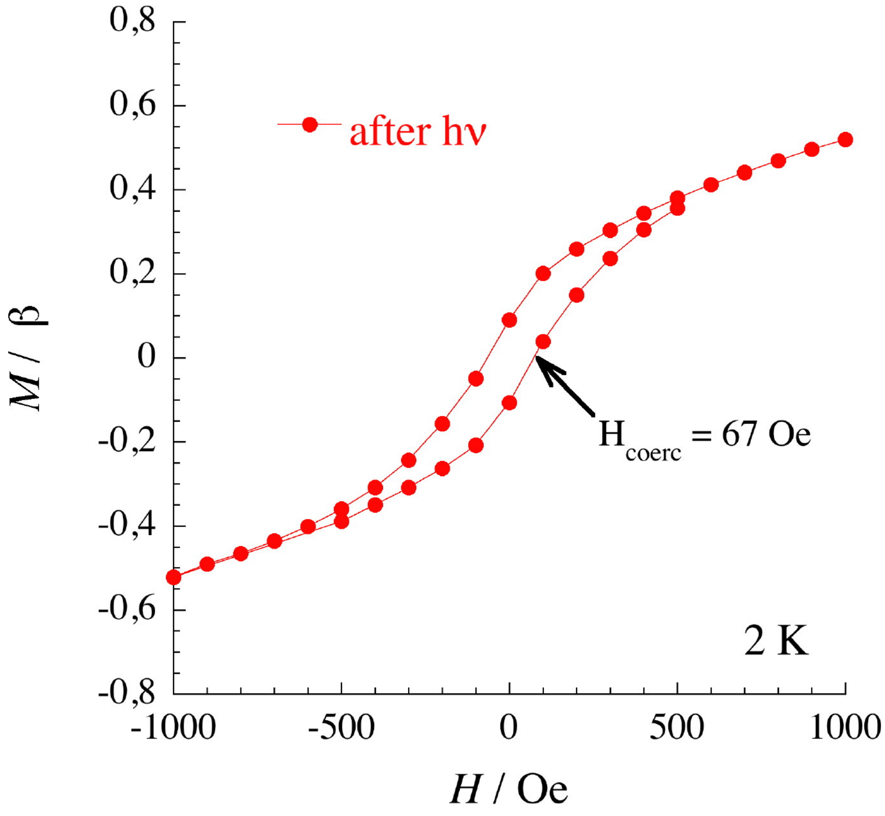

Fig. S14. M = f (H) at T = 2 K on the CsMoCu_DODA (top) and CsMoCu_PVP (bottom) samples after irradiation.

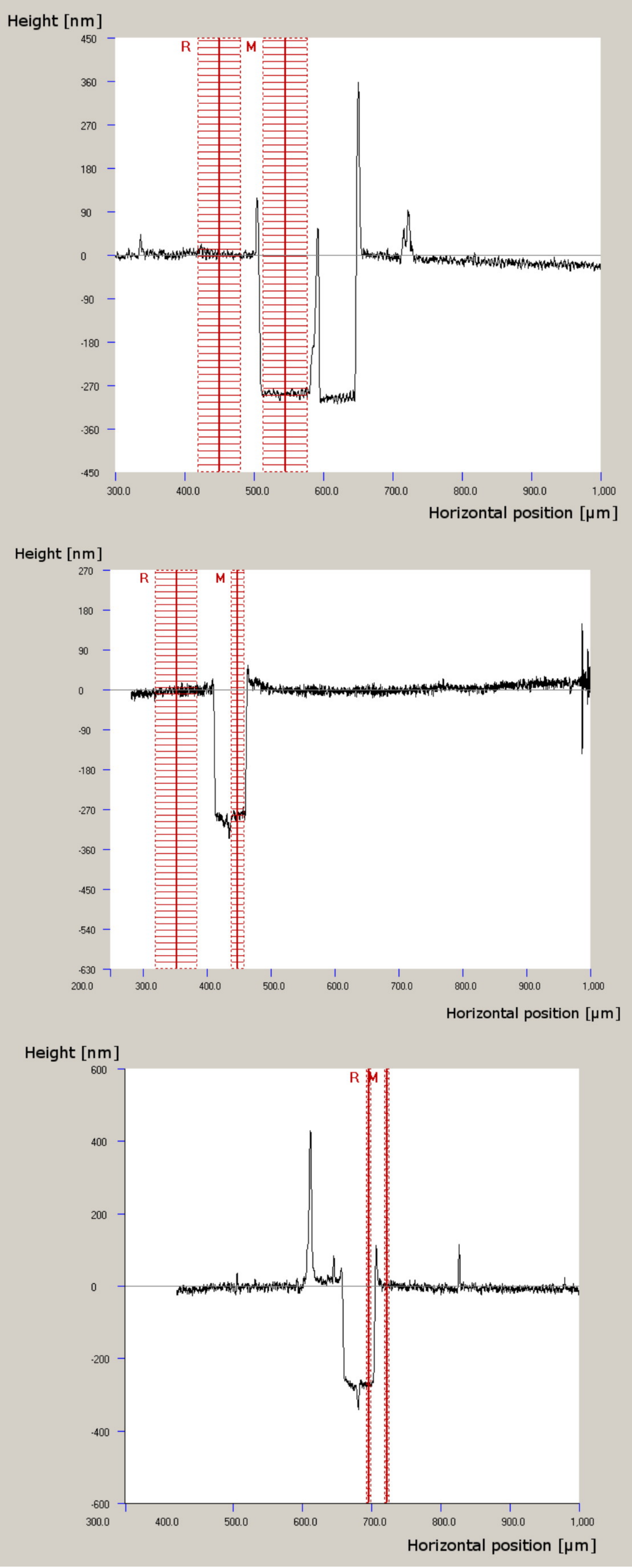

Fig. S15. Thickness profiles on three zones of a LB film with 119 monolayers (60 dipping cycles) of the CsMoCu nanoparticles deposited on a glass substrate.

The thickness measurements have been performed on a LB film prepared on a glass substrate after 60 dipping cycles while the sample for magnetic measurements was deposited on a mylar substrate after 45 dipping cycles (one dipping cycle comprises one immersion and withdrawal of the substrate). Unfortunately, it was not possible to evaluate the thickness directly of the LB film used for the magnetic measurements as the softness of the mylar substrate prevents the use of the profilometer that requires a hard substrate as a reference. The thickness was determined on three different points of the film, leading to a mean value of 280 nm (60 cycles). The resulting thickness shows average value of 4.7 nm per dipping cycle, and this would give a thickness of 210 nm for the LB film used for magnetic measurements (45 dipping cycles). The expected structure for a perfect layer-by-layer growth could be formed by bilayers of DODA alternating with monolayers of nanoparticles as observed in LB films of large polyoxometalate anions and DODA [1] with one bilayer of DODA and one monolayer of the particles deposited for each dipping cycle. Considering a height of 10 nm for the particles and 3 nm for the bilayer DODA shell, this gives about 16 layers of particles instead of the expected value of 45. This not perfect layer-by-layer growth can be basically attributed to the uncompleted coverage for each monolayer, already observed by AFM in the LB films with 1, 5 and 9 monolayers.

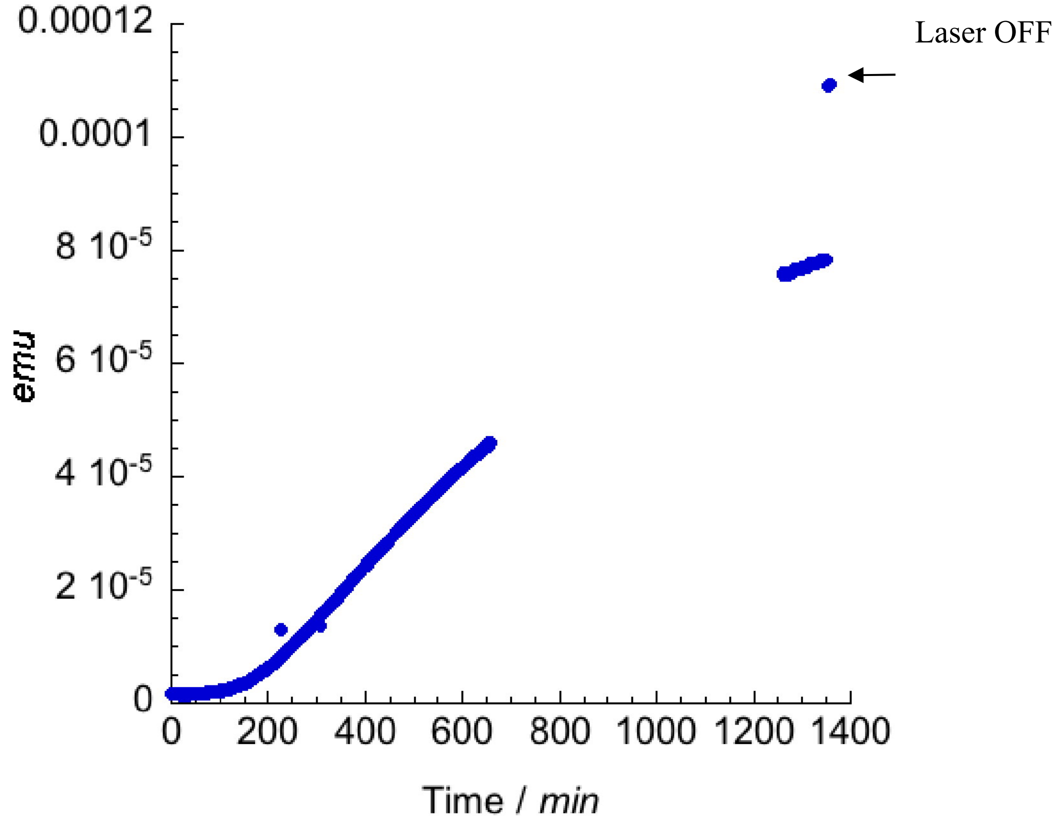

Fig. S16. Kinetic evolution of the magnetization during irradiation at 10 K under 100 Oe for the CsMoCu_DODA sample.

[1] M. Clemente-León, T. Ito, H. Yashiro, T. Yamase, *Chem. Mater.* **2007**, *19*, 2589